

**Artigo Original****The Burden of Senescent Dysfunctional Telomeres in Normal Cells – a Pilot Study**

A Sobrecarga de Telômeros Disfuncionais em Células Normais – um Estudo Piloto

<http://dx.doi.org/10.18316/sdh.v10i1.8280>Vivian Francilia Silva Kahl<sup>1\*</sup> ORCID: 0000-0002-7615-8694**ABSTRACT**

**Introduction:** Dysfunctional telomeres are critical for human health. They can be identified by their length, prevalence of telomeric variant repeats and frequency of damage localised to the telomeres, marked by the presence of  $\gamma$ -H2AX. **Material and Methods:** Using the metaphase Telomere dysfunction-Induced Foci (mTIF) assay, this study investigated the presence of TCAGGG, a telomeric variant repeat, and its association with the canonical repeat (TTAGGG) in a human cancer cell line (HT1080) and a normal cell strain (MRC-5) overtime (120 days). **Results:** Due to cell growth arrest that accompanies cellular senescence, MRC-5 late population doublings (PD) show particularly short telomere length (TL) when compared to HT1080 in any stage and to MRC-5 early PD. Cancer cells displayed higher levels of TCAGGG, both alone and colocalised to the canonical repeat. HT1080 and MRC-5 late PD cells showed increased levels of  $\gamma$ -H2AX colocalised to the canonical, to the variant repeat, and to both canonical and variant combined, when compared to MRC-5 early PD. **Conclusion:** This pilot study identified that the fibrosarcoma cell line HT1080 is more susceptible to telomeric variant repeats occurrence, while normal late cells display higher levels dysfunctional telomeres, characterised by shorter TL and increased  $\gamma$ -H2AX presence.

**Keywords:** Telomere;  $\gamma$ -H2AX; Telomere Dysfunctional Induced Foci (TIF); Telomere Variants; Senescence.

**RESUMO**

**Introdução:** Telômeros disfuncionais são críticos para a saúde humana. Eles podem ser identificados

---

<sup>1</sup> The University of Queensland Diamantina Institute, The University of Queensland, Australia

\***Autor Correspondente:** The University of Queensland Diamantina Institute, Woolloongaba, QLD 4102, Australia.

**E-mail:** [vivian.kahl@gmail.com](mailto:vivian.kahl@gmail.com)

pelo seu comprimento, pela prevalência de variantes nas repetições teloméricas e pela frequência de danos localizados nos telômeros, marcados pela presença de  $\gamma$ -H2AX. **Materiais e Métodos:** Usando o ensaio de disfunção telomérica induzida (mTIF), esse estudo investigou a presença de TCAGGG, uma repetição telomérica variante, e sua associação com a repetição canônica (TTAGGG) em uma linhagem cancerígena (HT1080) e uma linhagem celular normal (MRC-5) humanas ao longo de um período (120 dias). **Resultados:** Devido à parada do crescimento celular que acompanha a senescência, as células MRC-5 em estágio final de duplicação de população (DP) apresentaram telômeros particularmente curtos quando comparadas às células HT1080 em qualquer estágio e à MRC-5 em estágio inicial de DP. Células cancerígenas exibiram elevados níveis da variante TCAGGG, tanto sozinha ou co-localizada com a sequência canônica. As linhagens HT1080 e MRC-5 em estágio inicial tiveram níveis de  $\gamma$ -H2AX aumentados quando co-localizados à sequência canônica, à sequência variante, e às duas sequências combinadas, quando comparadas com MRC-5 em estágio final. **Conclusão:** Este estudo piloto identificou que a linhagem de fibrossarcoma HT1080 é mais suscetível à ocorrência de variantes teloméricas, enquanto células normais em estágio final exibem mais altos níveis de telômeros disfuncionais, indicados por telômeros mais curtos e presença aumentada de  $\gamma$ -H2AX.

**Palavras-chave:** Telômeros;  $\gamma$ -H2AX; Ensaio De Disfunção Telomérica Induzida; Variantes Teloméricas; Senescência.

## INTRODUCTION

Human telomeres are nucleoprotein structures composed mainly by the 5'-TTAGGG-3' array repeats that terminates in a nucleotide overhang of the G-rich sequence<sup>1</sup>. Telomeres are associated to a six-protein complex called shelterin. The components of shelterin (TRF1, TRF2, POT1, TIN2, TPP1 and Rap1) specifically localize to telomeres and enables cells to distinguish chromosomes natural ends from DNA breaks, represses DNA repair reactions and regulates telomere maintenance mechanisms (TMM)<sup>2</sup>. Structurally, the 3'-overhang invades the duplex telomeric repeat forming telomere loops (t-loops), that sequesters the chromosome end, providing protection of the telomeres by hiding them from DNA damage repair (DDR) machinery<sup>3,4</sup>.

Telomeres represent an initial barrier against tumorigenesis as they shorten within each round of cell division, triggering cellular senescence<sup>5</sup>. However, as some cells are capable of bypass senescence, they can activate a TMM and become immortal. It has been shown that substantial or aberrant telomere loss can trigger cellular senescence, apoptosis, and/or genomic instability<sup>5-7</sup>. Therefore, telomere length (TL) has been actively investigated as a surrogate for oncogenesis indication and human ageing. Although TL alone is an important indicative of human health, telomere dysfunction is affected by other factors that not only its length. Disruption of t-loops, interference with shelterin components required to its formation and maintenance, loss of the G-overhang itself, or critically short tracts of TTAGGGn can lead to telomere dysfunction<sup>8</sup>.

In the recent years, literature has indicated that telomeres are not purely composed of the TTAGGG array<sup>9,10</sup>. The distal termini of telomeres comprise homogeneous arrays of the TTAGGG tract, whereas the most proximal 2-kb region contains a distribution of degenerate variants and canonical repeats<sup>8</sup>. Although is speculated that the structurally variant telomere-adjacent DNA regions vary depending on the chromosome end and cell type, their identity, abundance, extension, and distribution is still not fully characterised. Extremely short telomeres show higher arrangements of telomeric repeat variants, most likely due to a majority proportion of subtelomeric repeat elements present and t-loop loss<sup>11,12</sup>.

The importance of understanding the frequency and the structure of the variant repeats at the telomeres is that, as shorter as the canonical repeats' tracts are, the harder it is for the shelterin complex to properly bind to the telomeric region, compromising the t-loop formation, culminating in telomere deprotection<sup>2,8,12,13</sup>. To the date, only a few studies have investigated telomeric variants, and the ones that did it were focused on the potential different variants occurrence between telomerase-positive and alternative lengthening of telomeres (ALT) cell lines<sup>9,10,14</sup>. Authors were able to show that cells that utilise

ALT generate variant repeats differently from the cells that utilise telomerase<sup>9,10</sup>. To our knowledge, this is the first study investigating the prevalence of telomere dysfunction foci in telomeric variant repeats. We assessed the combination of those two patterns of telomere disturbance in both cancer and normal cell lines. Our pilot study identified increased presence of variant telomeric repeats accompanied by higher levels of telomere damage in normal cells under senescence, surpassing the damages observed in cancer cells.

## **MATERIAL AND METHODS**

### ***Cell culture***

The cell line HT1080 was cultured and maintained in Dulbecco's Modified Eagle's Medium (DMEM) (Gibco, Paisley, UK) with 10% of foetal bovine serum (FBS) at 37°C in 10% CO<sub>2</sub>. MRC-5 cell strain was cultured and maintained in alpha Dulbecco's Modified Eagle's Medium (αDMEM) (Gibco, Paisley, UK) with 10% FBS at 37°C in 5% CO<sub>2</sub>. Cells were harvested with Trypsin-EDTA (Gibco, Paisley, UK) and pelleted for further DNA extraction or pelleted and resuspended for cytogenetic analysis, as described below.

### ***Genomic DNA isolation***

Genomic DNA was isolated using the QIAamp DNA Kit (Qiagen, Marylan, USA), following the manufacturer's protocol. DNA concentration and quality were assessed by NanoDrop™ ND-2000 Spectrophotometer (Thermo Scientific, Norwood, Australia).

### ***Telomere length measurement***

Telomere real time quantitative polymerase chain reaction (qPCR) was performed relative to a single copy gene, HBG, as previously described<sup>15</sup>. Briefly, a standard curve was established using a human genomic DNA (gDNA, Roche, Mannheim, Germany). Final qPCR reactions consisted of 2x PowerUp™ SYBR™ Green Master Mix (Applied Biosystems, Mulgrave, Australia); 500 nM of telomere primers forward and reverse or 300 nM and 500 nM of HBG primers forward and reverse, respectively; and 5 ng of DNA. The telomere primers sequences used in this study were: F: 5'- CGG TTT GTT TGG GTT TGG GTT TGG GTT TGG GTT TGG GTT TGG GTT -3' and R: 5' – GGC TTG CCT TAC CCT TAC CCT TAC CCT TAC CCT TAC CCT – 3', while the HBG primers were: F: 5'- GCT TCT GAC ACA ACT GTG TTC ACT AGC -3' and R: 5' – CAC CAA CTT CAT CCA CGT TCA CC -3'<sup>15</sup>. Results were expressed relative to U-2 OS cell line DNA and presented as telomere/single copy gene ratio (T/S ratio; arbitrary units). Experiments were carried out in a QuantStudio™ 5 Real-Time PCR System (Applied Biosystems, Mulgrave, Australia) and analysed using QuantStudio™ Design and Analysis Desktop Software (Applied Biosystems, Mulgrave, Australia).

### ***Metaphase telomere dysfunction-induced foci (mTIF) assay***

Immunofluorescence and telomere fluorescence *in situ* hybridisation (FISH) were performed on metaphase spreads of HT1080 and MRC-5 cells, following the protocol described by Rai and Chang<sup>16</sup>. Cultured cells were treated with 20 ng/mL of KaryoMAX™ Colcemid™ solution (Thermo Scientific, Norwood, Australia) for 2 hours, harvested using Trypsin-EDTA (Gibco, Paisley, UK), and resuspended in KCl-trisodium citrate buffer. Cell solution was cytocentrifuged onto microscope glass slides at 450 xg for 10min, fixed with 4% formaldehyde in 1x PBS, permeabilised in KCM buffer, and blocked with 100 µg/mL of DNase-free RNase A (Sigma-Aldrich, Castle Hill, Australia). The glass slides were incubated with γ-H2AX primary antibody (Cat n. 2893, Abcam, Cambridge, England), washed with 1x PBST, incubated

with Alexa Fluor 488 secondary antibody (Cat n. A32790, Invitrogen, Norwood, Australia), and washed again with 1x PBST. Subsequently, the slides were dehydrated in a graded ethanol series (70%, 90%, 100%) for 3min each, followed by an incubation with the combination of the canonical and variant PNA telomeric probes (TAMRA-OO-KKK(TTAGGG)<sub>3</sub> and FAM-OO-(TCAGGG)<sub>3</sub>; Panagene, Daejeon, South Korea). The incubation included a 3min step at 80° followed by hybridisation at room temperature overnight. Slides were then washed in 70% (v/v) formamide and 10mM Tris and with 50mM Tris, 150mM NaCl and 0.08% (v/v) Tween-20, rinsed in deionized water and air dried. Slides were finally mounted in ProLong™ Gold antifade reagent with DAPI (Invitrogen, Carlsbad, USA), imaged on a Zeiss Axio Imager microscope at 63x and analysed with Zen v2.3 Pro software (Carl Zeiss, North Ryde, Australia).

## Statistical analysis

Graphs and statistical analysis were generated using GraphPad Prism v8.4.3. Normality of data was tested using the Kolmogorov-Smirnov test. Normally distributed data was analysed using two-sided Student's *t*-test, while the two-sided Mann-Whitney test was performed on data assumed to be non-normally distributed. A *p* value of < 0.05 was considered statistically significant. Further details of statistical analyses are provided in the figure legends.

## RESULTS

This study assessed the telomere biology profile of a cancer cell line and a normal cell strain overtime. HT1080 is a fibrosarcoma cell line, that utilises telomerase as TMM<sup>17</sup>. MRC-5 is a normal human fibroblast cell strain that lacks a TMM, leading to telomere attrition<sup>18</sup>.

The HT1080 cell line was cultivated for 80 days, in which cells went from 22 population doublings (PD) to 101 PDs (Figure 1A,B). As a normal cell strain, MRC-5 cells grow slower than cancer cells, and to achieve a senescence period, they require a longer growing period<sup>5,18</sup>. They were cultivated for 120 days, going from PD 20 to PD 50 only (Figure 1C,D). To confirm the senescence triggering, we stained the MRC-5 cells in both early (PD20) and late (PD50) stages with  $\beta$ -galactosidase ( $\beta$ -gal), a marker of cellular senescence<sup>19</sup> (Figure 1E,F). Senescence was visually confirmed by both low cell confluency and blue staining (Figure E) and by  $\beta$ -gal cell-stained counting (Figure 1F). From the 200 cells scored for each MRC-5 early and late PDs, only 3% were stained with  $\beta$ -gal in the early stage, while 91% were stained with  $\beta$ -gal in the late stage ( $p < 0.0001$ ; Mann-Whitney test).

Next, we assessed telomere length (TL) by qPCR in both HT1080 and MRC-5 cells in early and late PDs (Figure 2). There was no significant difference of TL between HT1080 early and late PDs ( $p = 0.391$ ; Student's *t*-test), but both stages of HT1080 had shorter TL than MRC-5 early PD ( $p < 0.05$  for both HT1080 PDs; Student's *t*-test), and longer than MRC-5 late PD ( $p < 0.01$  and  $p < 0.001$  for HT1080 early and late PDs, respectively; Student's *t*-test). The telomere dynamics overtime in MRC-5 denotes the normal telomere attrition rates, until senescence triggering (Figure 2). Due to cell growth arrest that accompanies cellular senescence (Figure 1 C, D), MRC-5 late PD shows particularly short TL (Figure 2) when compared to HT1080 in any stage and to MRC-5 early PD ( $p < 0.0001$ ; Student's *t*-test).

**Figure 1.** Characterisation of the cell lines utilized in this study. **(A)** Cell growth and population doublings for HT1080; **(B)** Representative images of HT1080 cell line in the day 20 and day 80 (last day) of cell culture; **(C)** Cell growth and population doublings for MRC-5 cell strain; **(D)** Representative images of MRC-5 normal cell strain in the day 20 and day 120 (last day) of cell culture; **(E)** Representative images of MRC-5 fibroblasts stained with senescence associated  $\beta$ -galactosidase at early (day 20) and late (day 120) population doublings; **(F)** Quantitation of  $\beta$ -galactosidase staining in 200 cells for each MRC-5 population doublings.

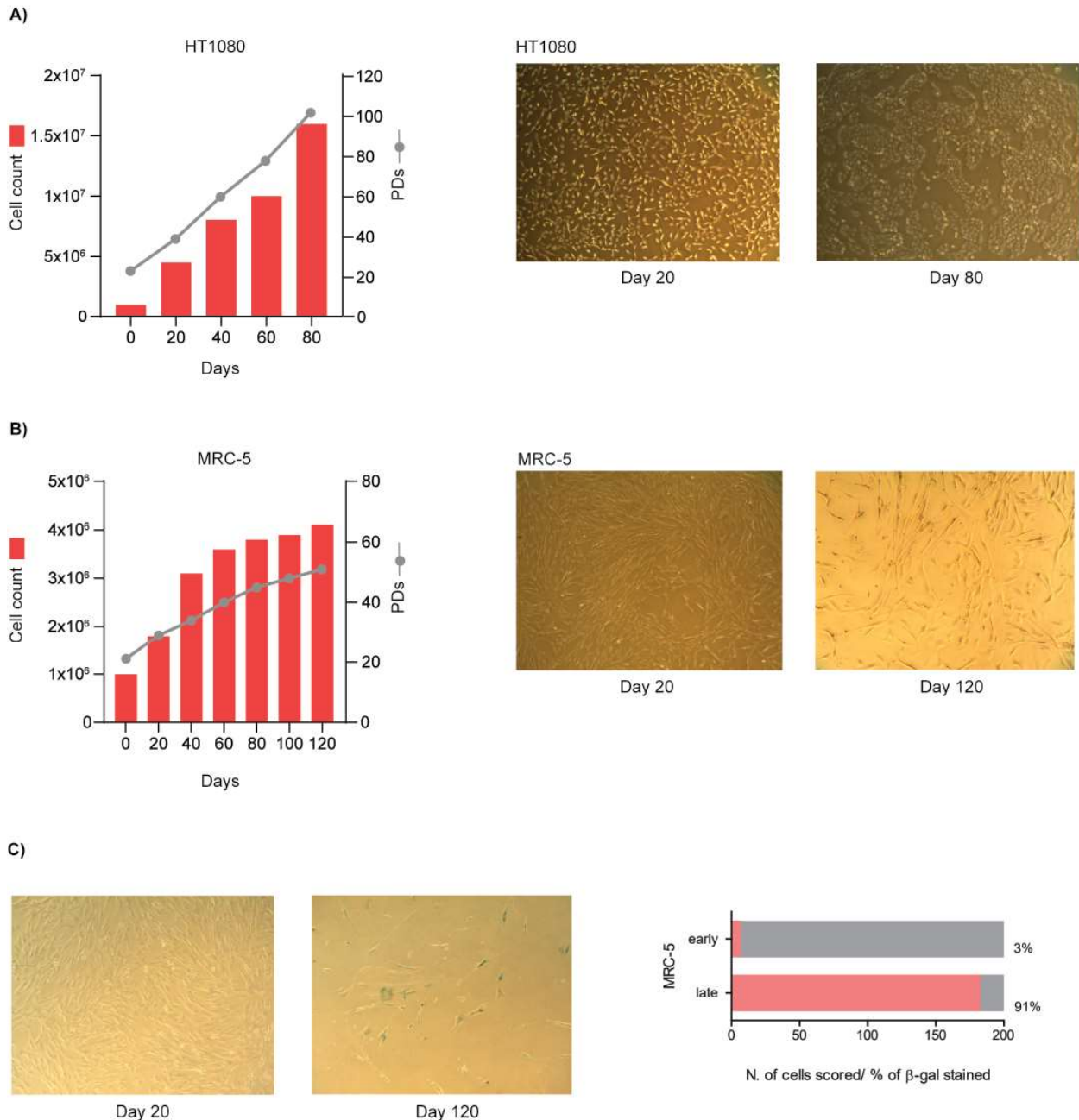
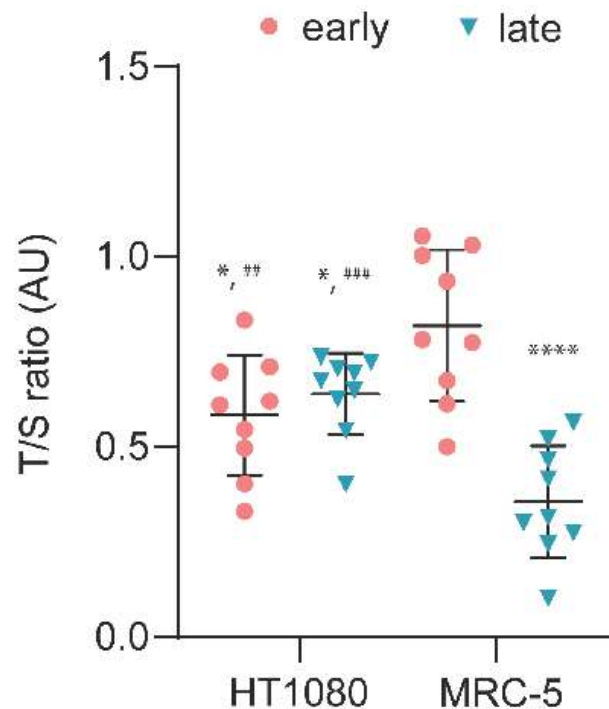


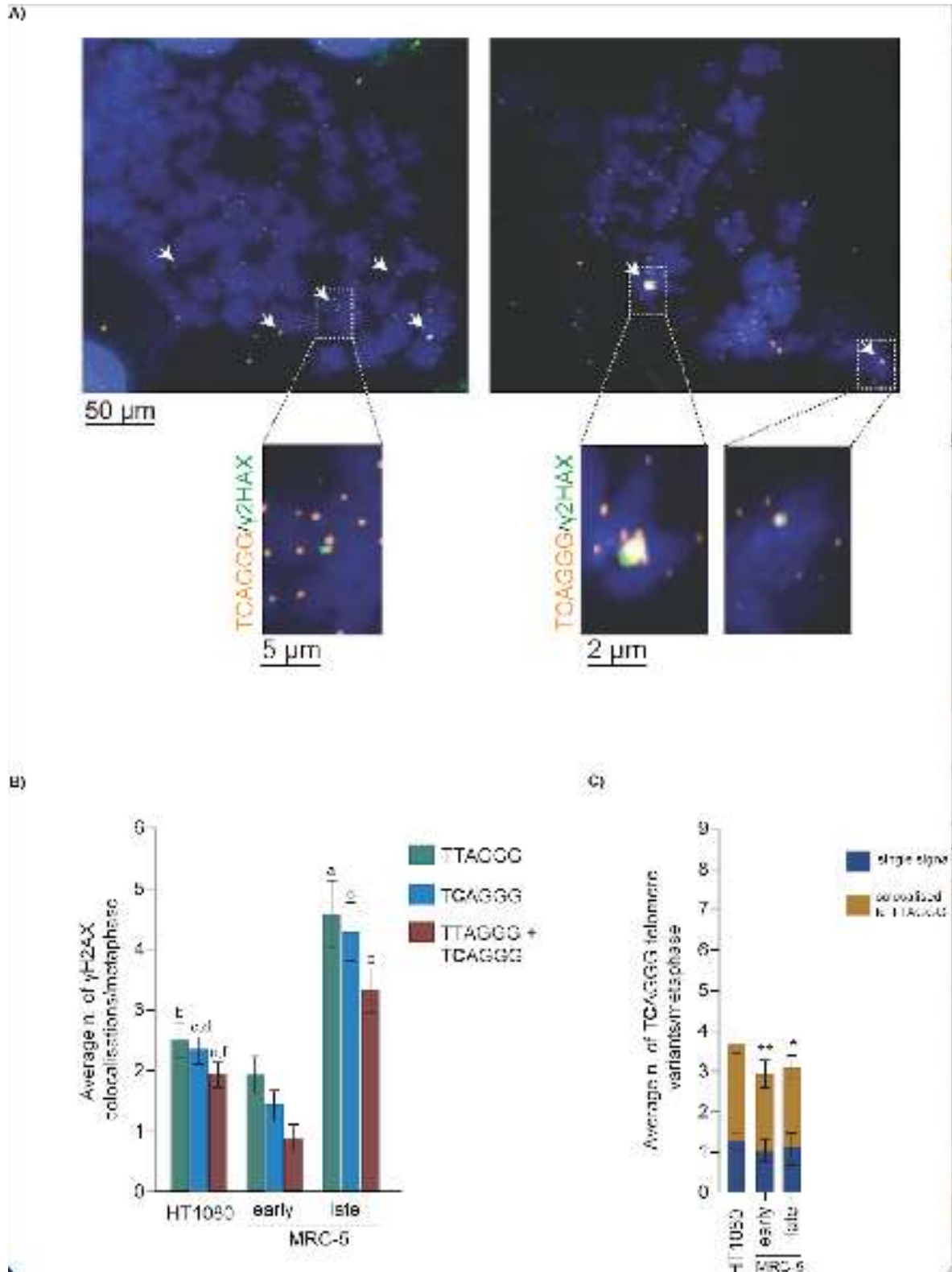
**Figure 2.** Scatter plot of telomere length measurement assessed by qPCR in HT1080 and MRC-5 cell lines in early and late population doublings (PD). Data presented as T/S ratio in arbitrary units (AU). Error bars are mean  $\pm$  SEM from  $n = 3$  technical replicates from 3 independent experiments, \* $p < 0.05$  and \*\*\*\* $p < 0.0001$  in relation to MRC-5 early PD, ## $p < 0.01$  and #### $p < 0.001$  in relation to MRC-5 late PD. Student  $t$ -test.



Finally, we used the mTIF assay to quantitatively measure telomere dysfunction in HT1080 and MRC-5 cells (Figure 3). The mTIF assay detects colocalization of telomeres and DNA damage response (DDR) markers, such as phosphorylated gamma-H2AX ( $\gamma$ -H2AX) in TIFs<sup>16,20</sup>. Fig 3A is a representative image of the metaphases scored, and it shows the colocalization of  $\gamma$ -H2AX with the telomeric PNA probe that labels the variant sequence TCAGGG in metaphase spreads. For mTIF assay, the HT1080 cell line was assessed only on its late PD, while MRC-5 cells were assessed for both early and late PDs. In average, the number of colocalization between  $\gamma$ -H2AX and TTAGGG was higher than all other combinations, while the lower was between  $\gamma$ -H2AX and both TTAGGG + TCAGGG together (Figure 3B) for all cell lines and PDs analysed. Interestingly, when compared to MRC-5 early PD, HT1080 and MRC-5 late PD showed increased average of  $\gamma$ -H2AX with TTAGGG ( $p < 0.0001$  and  $p < 0.0001$ , respectively; Mann-Whitney test), with TCAGGG ( $p < 0.0001$  for both; Mann-Whitney test) and with combined TTAGGG + TCAGGG ( $p < 0.0001$  for both; Mann-Whitney test; Figure 3B). Moreover, the late PD of MRC-5 displayed a strikingly increased in colocalization of TIFs by at least 2.5-fold than MRC-5 early (Figure 3B). In average, we observed 4.5 TIFs in TTAGGG metaphases, 4 TIFs in TCAGGG metaphases and 3.2 TIFs in TTAGGG + TCAGGG metaphases in MRC-5 late PD. In contrast, the next higher number of TIFs was observed in the TTAGGG metaphase of the HT1080 cell line, with an average of 2.5 (Figure 3B).

We also scored the average number of TCAGGG telomeric variant per metaphase, either found as a single signal at the end of the chromosomes or colocalised with the canonical sequence, TTAGGG (Figure 3C). No significant differences were observed between the sample set for TCAGGG single signal. The average single TCAGGG was around 1.2 among HT1080, MRC-5 early and late PDs (Figure 3C). We observed a significant increase of TCAGGG colocalised to TTAGGG presence in HT1080 when compared to MRC-5 early PD ( $p < 0.01$ ; Mann-Whitney test) and late PD ( $p < 0.05$ ; Mann-Whitney test).

**Figure 3.** mTIF in HT1080 cell line and early and late population doublings (PD) of MRC-5 cell strain. **(A)** Representative image of mTIF assay performed in HT1080 cell line stained with  $\gamma$ -H2AX immunofluorescence (green), telomere FISH (orange) and DAPI (blue). Scale bars: 50 $\mu$ m. Magnified images show the colocalization of  $\gamma$ -H2AX with TCAGGG variant repeat. Scale bars: 5 $\mu$ m and 2 $\mu$ m. mTIFs are indicated by white arrows. **(B)** Average abundance of  $\gamma$ -H2AX colocalised to TTAGGG, TCAGGG and TTAGGG + TCAGGG combined for HT1080 and MRC-5 metaphases. Error bars are mean  $\pm$  SEM from  $n =$  at least 150 metaphases scored per cell line and stage.  $a p < 0.001$  and  $b,c,e p < 0.0001$  in relation to MRC-5 early PD under the same telomeric variant condition;  $d,f p < 0.0001$  in relation to MRC-5 late PD under the same telomeric variant condition. Student  $t$ -test. **(C)** Average number of TCAGGG variant per metaphase, either scored as single signal or colocalised to TTAGGG. Error bars are mean  $\pm$  SEM from  $n =$  at least 150 metaphases scored per cell line and stage. \*  $p < 0.05$  and \*\*  $p < 0.01$  in relation to HT1080 for TCAGGG colocalised to the canonical repeat. Student  $t$ -test.



## DISCUSSION

Telomere length plays an important role in senescence triggering. Evidence points out that both shortening and lengthening of telomeres are related to their variant repeats<sup>9,21</sup>. Furthermore, stable and homogeneous TL provides the substrate for shelterin access to telomeres, leading to the proper formation of stable t-loops<sup>3,4,11,12</sup>. Our pilot study investigated telomere dysfunction using the mTIF and FISH assays. We observed that normal senescent cells display highly dysfunctional telomeres, even when compared to a cancer cell line.

Telomere length has been shown to have a negative correlation with chronological age and is considered a substantial indicator of lifetime health<sup>22-24</sup>. We followed up a cancer cell line (HT1080) and a mortal cell strain (MRC-5) during 80 and 120 days, respectively. This approach allowed us to investigate telomere dynamic changes overtime in cells with normal telomere attrition rates, until the senescence triggering (approximately PD50)<sup>7</sup>, as evident by senescence associated  $\beta$ -galactosidase present in MRC-5 late PDs. Due to the cell growth arrest that accompanies cell senescence, MRC-5 PD50 shows particularly short TL. Literature shows that the average TL loss per cell division in cells lacking TMM is approximately 70 bp/cell division<sup>22</sup>. The HT1080 fibrosarcoma cell line grew exponentially for 80 days, going from PD22 to PD 101, displaying a faster grow than the normal cell strain. The long culture period did not affect cells confluency as well. Moreover, there was no significant differences for TL between HT1080 early and late PDs. This highlights at least four out of the six known hallmarks of cancer: resisting cell death, sustaining proliferative signalling, evading growth suppressors and enabling replicative immortality<sup>25</sup>.

Until recently, the TTAGGG canonical repeat had been considered the only characteristic sequence of the telomeric region. The most proximal 2-kb region of human telomeres, i.e., nearly invasion to the subtelomeric region, contains a random distribution of variants and canonical repeats. They are in linkage disequilibrium and have evolved along haploid lineages<sup>2,26</sup>. Although the distal ends of the chromosome comprise homogeneous arrays of TTAGGG sequence, recent evidence point out that the variant repeats can occur throughout the distal ends as well, particularly due to genomic instability, homologous recombination at telomeres, and senescence triggering<sup>2,7,9,10,12</sup>. Dysfunctional telomeres are the first step to carcinogenesis<sup>5</sup>.

We used the FISH assay along with mTIF to identify potential frequencies of the variant TCAGGG colocalised to the TTAGGG canonical repeats versus the frequency of TTAGGG alone. Sequence variants are supposedly added along with the canonical sequence, as cells would be under significantly DNA damage and most likely display massive cell death if only variants were incorporated<sup>10,14</sup>. Yet, we observed the occurrence of only TCAGGG in our sample set, although in a much lower ratio than when colocalised to TTAGGG. A study from 2012 also observed a higher number of variants in both ALT and telomerase positive cell lines. In fact, only around 55% of all telomeric sequence were composed by the canonical sequence, while the remaining was distributed among different variant types<sup>10</sup>. Kim et al.<sup>14</sup> observed revoking of telomeres in mouse ALT cells with non-telomeric sequences. Noteworthy, we did not include any ALT cell line in our study, only a telomerase positive one (HT1080), which is a limitation of the current study. HT1080 cells displayed higher average of TTAGGG/TCAGGG colocalization than both MRC-5 early and late PDs. Moreover, the relative lower canonical sequence purity observed in MRC-5 cell strains, particularly in PD50, agrees with the known increase in telomeric variant repeats due to senescence<sup>27,28</sup>.

The increase in telomere sequence variants is associated with disruption of shelterin components, particularly TRF2 and POT1, which also increases the occurrence of TIFs<sup>2,4,29,30</sup>. The deletion of POT1 and TRF2 activates DDR in telomeres through two different pathways: while TRF2 engages ATM, POT1 depletion activates the ATR pathway. TIFs also occur under p-53 mediated cellular arrest, induction of nonhomologous end joining (NHEJ)-dependent end-to-end chromosome fusions, among others<sup>20,31-33</sup>. All those situations recruit  $\gamma$ -H2AX to telomeres<sup>2</sup>.

This study identified the occurrence of  $\gamma$ -H2AX at the chromosome ends of HT180 cell line with no differences between colocalised to TTAGGG, to TCAGGG or to both sequences together. In terminally-differentiated tissues of old primates, DDR markers accumulate at telomeres which are not critically short<sup>34</sup>, as in the case of HT1080 observed here. On the opposite, MRC-5 early PD had significant lower levels of  $\gamma$ -H2AX in all colocalizations combinations and of TCAGGG variant repeats, either alone or colocalised to the canonical sequence. Linear telomeric DNA of normal cells induces a prolonged checkpoint, being not uniformly repaired. Telomeric tracts, if damaged, are irreparable and can trigger persistent DDR and cellular senescence<sup>34</sup>. The striking observation of this pilot study comes from this concept: late PD MRC-5 cell displayed a significant increase average of TIFs per metaphase in relation to early MRC-5 cells and to HT1080. This data is consistent with literature showing spontaneous telomere dysfunction in normal human cells, in which the presence of only five TIFs indicates the onset of cellular senescence<sup>7</sup>. MRC-5 PD50 exhibited markers of replicative senescence, including cell growth arrest, altered cell morphology, increased numbers of  $\beta$ -galactosidase-positive cells and telomere shortening.

An enabling characteristic of the hallmarks of cancers is genome instability and mutations. Genomic instability at telomeres can lead to the loss of the telomeric repeats more rapidly than just normal senescence<sup>25</sup> and to the recruitment of DDR factors to the telomeres. This pilot study showed that normal cells with dysfunctional telomeres display characteristics of senescence triggering, as expected, but that some of them (i.e., DNA damage at telomeres) are even more pronounced than in cancer cells. We also identified that although late normal cells have more telomeric dysfunctional, cancer cells, i.e., a fibrosarcoma, are more susceptible to telomeric variants occurrence. We acknowledge that further studies are needed to confirm our findings, and especially, studies including ALT cells and different normal strains cells as well.

## Contributions

VFSK: Study design, experiment performance, data analysis, statistical analysis and manuscript writing.

## Declaration of interest

The author declares no conflict of interest.

## REFERENCES

1. Wright WT, Tesmer VM, Huffman, KE, Levene, SD, Shay JW. Normal human chromosomes have long G-rich telomeric overhangs at one end. *Genes & Development*. 1997 Nov 1; 11(21): 2801-2809. DOI: [10.1101/gad.11.21.2801](https://doi.org/10.1101/gad.11.21.2801).
2. Palm W, de Lange T. How shelterin protects mammalian telomeres. *Annual Reviews of Genetics*. 2008; 42: 301-334. DOI: [10.1146/annurev.genet.41.110306.130350](https://doi.org/10.1146/annurev.genet.41.110306.130350).
3. Griffith JD, Comeau L, Rosenfield S, Stansel RM, Bianch A, Moss H, et al. Mammalian telomeres end in a large duplex loop. *Cell*. 1999 May14; 97(4): 503-514. DOI: [10.1016/s0092-8674\(00\)80760-6](https://doi.org/10.1016/s0092-8674(00)80760-6).
4. Van Ly D, Low RRJ, Frölich S, Bartolec TK, Kafer GR, Pickett HA, et al. Telomere loop dynamics in chromosome end protection. *Molecular Cell*. 2018 Aug16, 71(4): 510-525. DOI: [10.1016/j.molcel.2018.06.025](https://doi.org/10.1016/j.molcel.2018.06.025).
5. Reddel R. Senescence: an antiviral defense that is tumor suppressor? *Carcinogenesis*. 2010 Jan; 31(1): 19-26. DOI: [10.1093/carcin/bgp274](https://doi.org/10.1093/carcin/bgp274).
6. Allsop RH, Harley CB. Evidence for a critical telomere length in senescent human fibroblasts. *Experimental Cell Research*. 1995 Jul; 219(1): 130-136. DOI: [10.1006/excr.1995.1213](https://doi.org/10.1006/excr.1995.1213).

7. Kaul Z, Cesare AJ, Huschtscha LI, Neumann AA, Reddel RR: Five dysfunctional telomeres predict onset of senescence in human cells. *EMBO Reports*. 2011 Dec23; 13(1): 52-59. DOI: [10.1038/embor.2011.227](https://doi.org/10.1038/embor.2011.227).
8. Riethman H. Human subtelomeric copy number variations. *Cytogenetic and Genome Research*. 2008; 123(1-4): 244-252. DOI: [10.1159/000184714](https://doi.org/10.1159/000184714).
9. Lee MH, Hills M, Conomos D, Stutz MD, Dagg RA, Lau LMS, et al. Telomere extension by telomerase and ALT generates variant repeats by mechanistically distinct processes. *Nucleic Acid Research*. 2014 Feb; 42(3): 1733-1746. DOI: [10.1093/nar/gkt1117](https://doi.org/10.1093/nar/gkt1117).
10. Conomos DS, Stutz MD, Hills M, Neumann AA, Bryn TM, Reddel RR, et al. Variant repeats are interspersed throughout the telomeres and recruit nuclear receptors in ALT cells. *The Journal of Cell Biology*. 2012 Dec10; 199(6): 893-906. DOI: [10.1083/jcb.201207189](https://doi.org/10.1083/jcb.201207189).
11. Xu L, Blackburn EH. Human cancer cells harbor T-stumps, a distinct class of extremely short telomeres. *Molecular Cell*. 2007 Oct26; 28(2): 315-327. DOI: [10.1016/j.molcel.2007.10.005](https://doi.org/10.1016/j.molcel.2007.10.005).
12. McCafrey J, Young E, Lassahn K, Sibert J, Pastor S, Riethman H, et al. High-throughput single-molecule telomere characterization. *Genome Research*. 2017 Nov; 27(11): 1904-1915. DOI: [10.1101/gr.222422.117](https://doi.org/10.1101/gr.222422.117).
13. Shay JW, Wright WE. Telomeres and telomerase: three decades of progress. *Nature Reviews. Genetics*. 2019 May; 20(5): 299-309. DOI: [10.1038/s41576-019-0099-1](https://doi.org/10.1038/s41576-019-0099-1).
14. Kim C, Sung S, Kim J-S, Lee H, Jung Y, Shin S, et al. Telomeres reformed with non-telomeric sequences in mouse embryonic stem cells. *Nature Communications*. 2021 Feb 17; 12(1): 1097. DOI: [10.1038/s41467-021-21341-x](https://doi.org/10.1038/s41467-021-21341-x).
15. Cawthon RM. Telomere measurement by quantitative PCR. *Nucleic Acid Research*. 2002 May15; 30(10): e47. DOI: [10.1093/nar/30.10.e47](https://doi.org/10.1093/nar/30.10.e47).
16. Rai R, Chang S. Probing the Telomere Damage Response. In: Songyang Z. (eds). *Telomeres and Telomerase*. *Methods in Molecular Biology*. New York: Humana Press; 2017.
17. Pickett HA, Cesare AJ, Johnston RL, Neumann AA, Reddel RR. Control of telomere length by trimming mechanism that involves generation of t-circles. *EMBO Journal*. 2009 Apr8; 28(7): 799-809. DOI: [10.1038/emboj.2009.42](https://doi.org/10.1038/emboj.2009.42).
18. Dewhurst SM, Yao X, Rosiene J, Tian H, Behr J, Bosco N, et al. Structural variant evolution after telomere crisis. *Nature Communications*. 2021 Apr7; 12(1): 2093. DOI: [10.1038/s41467-021-21933-7](https://doi.org/10.1038/s41467-021-21933-7).
19. Dimri GP, Lee X, Basile G, Acosta M, Scott G, Roskelley C, Medrano EE, Linskens M, Rubelj I, Pereira-Smith O. A biomarker that identifies senescent human cells in culture and in aging skin in vivo. *Proceeding of the National Academy of Science of USA*. 1995 Sep26; 92(20): 9363-9367. DOI: [10.1073/pnas.92.20.9363](https://doi.org/10.1073/pnas.92.20.9363).
20. Cesare AJ, Kaul Z, Cohen SB, Napier CE, Pickett HA, Neumann AA, Reddel RR. Spontaneous occurrence of telomeric DNA damage response in the absence of chromosome fusions. *Nature Structural & Molecular Biology*. 2009 Dec; 16(12): 1244-1251. DOI: [10.1038/nsmb.1725](https://doi.org/10.1038/nsmb.1725).
21. Campbell PJ, Getz G, Korel JO, Stuart JM, Jennings JL, Stein LD, et al. ICG/TGA Pan-Cancer Analysis of Whole Genomes Consortium. Pan-cancer analysis of whole genome. *Nature*. 2020 Feb; 578(7793): 82-93. DOI: [10.1038/s41586-020-1969-6](https://doi.org/10.1038/s41586-020-1969-6).
22. Harley CB, Futcher AB, Greider CW. Telomeres shorten during ageing of human fibroblasts. *Nature*. 1990 May31; 345(6274): 458-460. DOI: [10.1038/345458a0](https://doi.org/10.1038/345458a0).
23. Baird DM. Telomere dynamics in human cells. *Biochimie*. 2008 Jan; 90(1): 116-121. DOI: [10.1016/j.biochi.2007.08.003](https://doi.org/10.1016/j.biochi.2007.08.003).
24. Shay JW. Role of telomeres and telomerase in aging and cancer. *Cancer Discovery*. 2016 Jun; 6(6): 584-593. DOI: [10.1158/2159-8290.CD-16-0062](https://doi.org/10.1158/2159-8290.CD-16-0062).

25. Hanahan D, Weinberg RA. Hallmarks of cancer: the next generation. *Cell*. 2011 Mar4; 144(5): 646-574. DOI: [10.1016/j.cell.2011.02.013](https://doi.org/10.1016/j.cell.2011.02.013).
26. Baird DM, Jeffreys AJ, Royle NJ. Mechanisms underlying telomere repeat turnover, revealed by hypervariable variant repeat distribution patterns in the human Xp/Yp telomere. *EMBO Journal*. Nov 1; 14(21): 5433-5443.
27. Alhendi ASN, Royle NJ. The absence of (TTAGGG)<sub>n</sub> repeats in some telomeres, combined with variable responses to NR2F2 depletion, suggest that this nuclear receptor plays an indirect role in the alternative lengthening of telomeres. *Scientific Reports*. 2020 Nov26; 10(1): 20597. DOI: [10.1038/s41598-020-77606-w](https://doi.org/10.1038/s41598-020-77606-w).
28. Uppuluri L, Varapula D, Young E, Riethman H, Xiao M. Single-molecule telomere length characterization by optical mapping in nano-channel array: Perspective and review on telomere length measurement. *Environmental Toxicology and Pharmacology*. 2021 Feb; 82: 103562. DOI: [10.1016/j.etap.2020.103562](https://doi.org/10.1016/j.etap.2020.103562).
29. Vinchure OS, Whitemore K, Kushwah D, Blasco MA, Kulshreshtha R. miR-490 supresses telomere maintenance program and associated hallmarks in glioblastoma. *Cell and Molecular Life Sciences*. 2021 Mar; 78(5): 2299-2314. DOI: [10.1007/s00018-020-03644-2](https://doi.org/10.1007/s00018-020-03644-2).
30. Li T, Luo Z, Lin S, Li C, Dai S, Wang H, Huang J, Ma W, Songyang Z, Huang Y. MiR-185 targets POT1 to induce telomere dysfunction and cellular senescence. *Aging*. 2020 Jul18; 12(14): 14791-14807. DOI: [10.18632/aging.103541](https://doi.org/10.18632/aging.103541).
31. Denchi EL, de Lange T. Protection of telomeres through independent control of ATM and ATR by TRF2 and POT1. *Nature*. 2007 Aug30; 448(7157): 1068-1071. DOI: [10.1038/nature06065](https://doi.org/10.1038/nature06065).
32. Guo X, Deng Y, Lin Y, Cosme-Blanco W, Chan S, He H, Yuan G, Brown EJ, Chang S. Dysfunctional telomeres activate an ATM-ATR-dependent DNA damage response to supress tumorigenesis. *EMBO Journal*. 2007 Nov14; 26(22): 709-4719. DOI: [10.1038/sj.emboj.7601893](https://doi.org/10.1038/sj.emboj.7601893).
33. Ruis P, Boulton SJ. The end replication problem – an unexpected twist in the tail. *Genes & Development*. 35: 1-21. DOI: [10.1101/gad.344044](https://doi.org/10.1101/gad.344044).
34. Fumagalli M, Rossiello F, Clerici M, Barozzi S, Cittaro D, Kaplunov JM, Bucci G, Dobрева M, Matti V, Beausejour CM, Herbig U, Longhese MP, d'Adda di Fagagna F. Telomeric DNA damage is irreparable and causes persistent DNA-damage-response activation. *Nature Cell Biology*. 2012 Mar18; 14(4): 355-365. DOI: [10.1038/ncb2466](https://doi.org/10.1038/ncb2466).